Mechanisms of Stereochemical Control in Propylene Polymerizations with Soluble Group 4B Metallocene/Methylalumoxane Catalysts

John A. Ewen

Contribution from the Long Range Polymer Group, Plastics Technology Division, Exxon Chemical Company, Baytown, Texas 77522. *Received March 12, 1984*

Abstract: The soluble bis(cyclopentadienyl)bis(phenyl)titanium/methylalumoxane catalyst system produces isotactic polypropylene with a novel stereoblock microstructure consistent with a chain-end stereochemical control mechanism. Chiral catalysts derived from the racemic enantiomers of ethylene-bridged indenyl derivatives are the first metallocene catalysts to form isotactic polypropylene with the conventional structure predicted by an enantiomorphic-site stereochemical control model. The meso achiral form of the ethylene-bridged titanium indenyl diastereomers and zirconocene derivatives produce polypropylene with an ideally atactic structure. Differing regiospecificities during cis addition with soluble Ti and V chain-end controlled stereospecific systems result in Ti being isotactic specific and V being syndiotactic specific.

Ziegler–Natta catalysts produce isotactic, syndiotactic, or atactic polypropylenes.[1-4] ^{13}C NMR analyses of the steric pentads of commercially important highly isotactic polypropylene produced with heterogeneous Ti(III)-based Ziegler–Natta catalysts are consistent with the the polymer having the configurational microstructure represented by the idealized structure I[5,6]

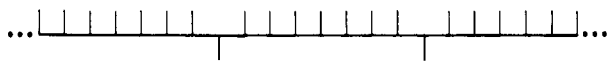

I

The pseudoasymmetric methine carbon atoms of successive monomer units have the same relative configuration with occasional placements of units with opposite handedness. The relative configurations of the adjacent pseudoasymmetric centers are used in NMR notation.[7] Structure I thus corresponds to ...mmmmmmrrmmmmmmrrmmmmmm..., i.e., stereosequences of isotactic meso (m) dyads connected by pairs of syndiotactic racemic (r) dyads. Simple statistical analyses of the distribution of the mr and rr steric triads for isotactic polypropylenes with structure I are consistent with an enantiomorphic-site propagation model based on stereochemical control by the chirality of the catalyst.[8,9]

On the other hand, pentad distributions of syndiotactic polypropylene produced with soluble V catalysts[10] (...rrrrmrrr...) obey the symmetric Bernoullian statistical model proposed by Bovey.[11] Syndiotactic polymerizations have thus, so far, been consistent with the asymmetry of the last inserted monomer unit controlling the stereochemistry of polymerization as opposed to the asymmetry of either the transition-metal or stereorigid ancillary ligands (...rrrmmrrr...) being the controlling factor.

Propylene polymerizations with group 4B bis(cyclopentadienyl)M(IV) derivatives (M = Ti or Zr) and methylalumoxane cocatalysts have yielded only atactic stereosequences in the past.[12,13] This paper deals with the first definitive examples of isotactic polypropylene obtained with soluble Ziegler–Natta catalysts, determination of the polymer stereochemical microstructures, and information concerning the reaction mechanism.

The bis(cyclopentadienyl)bis(phenyl)titanium-based system is shown to yield the first example of polypropylene with a ...mmmmmrmmmmmrmmmm... stereosequence, represented by the idealized structure II

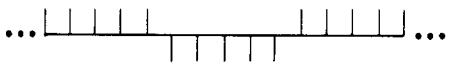

II

The pentad distributions of the polymers with structure II are in accord with the Bernoullian statistical model with stereochemical control by the configuration of the last inserted monomer unit. This mechanism results in propagation of the new chain-end configuration after a steric inversion.

Data are presented on ^{1}H NMR of isotopically labeled polypropylene, ^{13}C NMR analyses of low molecular weight polymer end groups, and ^{13}C NMR determinations of changes in the polymer microstructure on alteration of the stereochemistry of the active sites. It is concluded that polymerization occurs by "1–2" cis addition, retention of configuration at the coordinated carbon atom, predominant monomer coordination at a lateral coordination vacancy in the noncyclopentadienyl ligand equatorial plane,[14] and with the primary carbon atom of the last inserted monomer unit (position 1, by the IUPAC nomenclature[15]) bound to the transition metal.

Enantiomeric rac forms of analogous ethylene-bridged indenyl titanocene derivatives represent the first soluble metallocenes to produce polypropylene with a microstructure consistent with the enantiomorphic-site control structure represented by structure I. Atactic polypropylene is produced by the ethylene-bridged indenyl meso diastereomer and achiral zirconocene derivatives. Structural features of the reaction intermediates are inferred from the polymer microstructural responses to variations in the steric requirements and geometric arrangements of the cyclopentadienyl ligands.

Experimental Section

Reagents. Cp_2TiCl_2 and Cp_2ZrCl_2 were obtained from Strem Chemicals. $(Me_5Cp)(Cp)$ $ZrCl_2$ was prepared from stoichiometric amounts of $CpZrCl_3$[16] and Me_5CpLi in tetrahydrofuran at −78 °C under a N_2

(1) Ketley, A. D., Ed. "The Stereochemistry of Macromolecules"; Marcel Dekker: New York, 1967; Vol. 1.
(2) Keij, T. "Kinetics of Ziegler-Natta Polymerization"; Kadansha: Tokyo, 1972.
(3) Chien, J. C. W., Ed. "Coordination Polymerization"; Academic Press: New York, 1975.
(4) Boor, J., Jr. "Ziegler-Natta Catalysts and Polymerizations"; Academic Press: New York, 1979.
(5) Wolfsgruber, C.; Zannoni, G.; Rigamonti, E.; Zambelli, A. *Makromol. Chem.* **1975**, *176*, 2765.
(6) Doi, Y.; Suzuki, T.; Keii, T. *Makromol. Chem., Rapid Commun.* **1981**, *2*, 293.
(7) Stereochemical notation proposed by Frisch et al.: Frisch, H. L.; Mallows, C. L.; Bovey, F. A. *J. Chem. Phys.* **1966**, *45*, 1565.
(8) Doi, Y.; Asakuru, T. *Makromol. Chem.* **1975**, *176*, 507.
(9) Sheldon, R. A.; Fueno, T.; Tsunstsugu, T.; Kurukawa, J. *J. Polym. Sci., Part B* **1965**, *3*, 23.
(10) Zambelli, A.; Locatelli, P.; Provasoli, A.; Ferro, D. R. *Macromolecules* **1980**, *13*, 267.
(11) Bovey, F. A.; Tiers, G. V. D. *J. Polym. Sci.* **1960**, *44*, 173.
(12) Sinn, H.; Kaminsky, W. *Adv. Organomet. Chem.*, **1980**, *18*, 99.
(13) Pino, P.; Mulhaupt, R. *Angew. Chem., Int. Ed. Engl.* **1980**, *19*, 857.
(14) (a) Laulier, J. W.; Hoffman, R. *J. Am. Chem. Soc.* **1976**, *98*, 1729. (b) Ballhausen, C. J.; Dahl, J. P. *Acta Chem. Scand.* **1961**, *15*, 1333.
(15) Jenkins, A. D. *Pure Appl. Chem.* **1979**, *51*, 1101.

0002-7863/84/1506-6355$01.50/0

Scheme I[a]

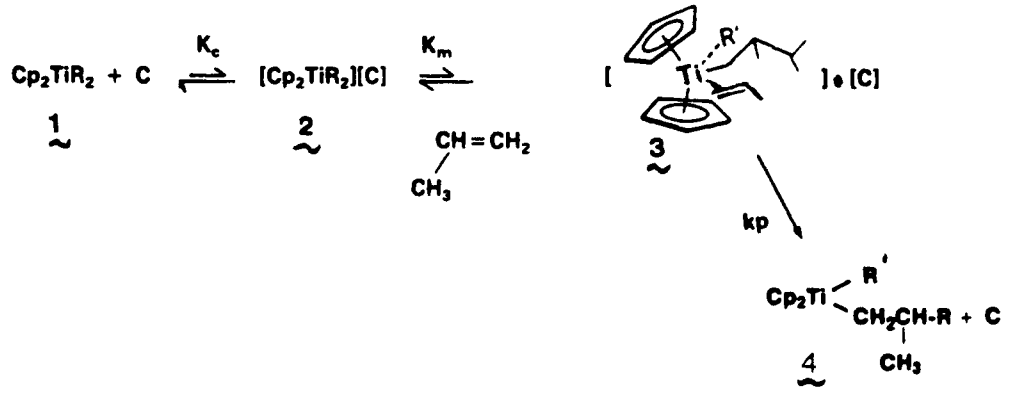

[a] Alumoxane = $[Al(CH_3)\text{-}O\text{-}]_n$-; represented as C.

atmosphere, purified by vacuum sublimation, and characterized by ^1H NMR. Bis(cyclopentadienyl)titanium diphenyl and diastereomers of (ethylene)bis(indenyl)titanium dichloride were prepared, purified, and characterized by reported procedures.[17] Isotopically labeled *cis*-CD_3CD_2=CHD was obtained from Merck Sharp and Dohme of Canada. Al stock solutions (1 m) which contained approximately a 1:1 mixture of methylalumoxanes and trimethylaluminum were prepared by cautiously adding 50 cm^3 of neat trimethylaluminum (Texas Alkyls) under a N_2 atmosphere to a slurry containing 500 cm^3 of toluene and $CuSO_4 \cdot 5H_2O$ (Aldrich Chemicals) (Al/H_2O = 1:1). The clear supernatant was decanted after the mixture was stirred for 8 h under N_2 at the reaction temperature. Standard vacuum line techniques and a Vacuum Atmospheres glovebox were used for preparation and storage of air-sensitive materials.

Polymerization. Polymerizations were performed in modified 1-L Zipperclaves obtained from Autoclave Engineers. Temperatures were maintained to within 1 °C of the desired temperature with externally circulated cold gaseous N_2 or thermostated H_2O. Reactions were initiated by injection of 5-cm^3 solutions of the catalyst contained in toluene into thermostated solutions containing measured amounts of purified toluene, propylene, and cocatalyst. The polymerization of isotopically labeled *cis*-CD_3CD_2=CHD in a glass vessel was cooled by an external isopropyl alcohol/liquid nitrogen slush bath. Polymerizations were stopped with with acidified methanol.

NMR Analysis. ^{13}C NMR spectra of the polymers were obtained by using 1,2,4-trichlorobenzene solvent at 135 °C in the Fourier transform (FT) mode on a Varian XL-200 spectrometer operating at 50.31 MHz. Field/frequency lock was established with Me_2SO-d_6 placed in a coaxial tube. Pentad chemical shift assignments were previously made[10,18,19] and are given in ppm relative to the chemical shift of the mmmm pentad. Instrument conditions were 60° pulse (13 μs), a 6.0-s repetition rate, and a 10000-Hz sweep depth. Five thousand transients were accumulated. ^1H NMR of the deuteriopolymers was recorded at 200 MHz with deuterium decoupling and with *o*-dichlorobenzene solvent and hexamethyldisiloxane (HMDS) internal standard. Tetrad chemical shifts are reported in ppm relative to the mmm tetrad.

GPC Analysis. GPCs of the polymers were recorded on a Waters Model 150C gel permeation chromatograph with five polystyrene gel columns (10^7-, 10^6-, 10^5-, 10^4-, and 10^3-Å pore sizes) and *o*-dichlorobenzene as solvent at 135 °C.

Results

$Cp_2Ti(Ph)_2$ Polymerization Kinetics. The polymerization rates were independent of time at −60 °C and exhibited the usual first-order dependencies on titanium and propylene.[2] An unusual feature of the kinetics is the rate dependency on aluminum concentrations to very high levels (Figure 1).

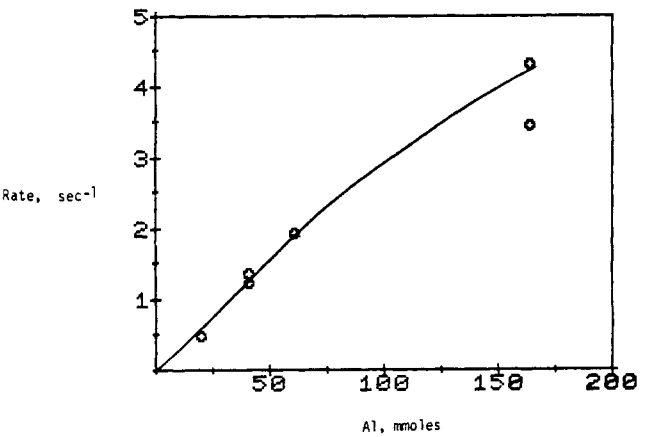

Figure 1. Integral polymerization rate dependence on concentration of total aluminum at −60 °C. Rate: moles of propylene consumed per mole of $Cp_2Ti(Ph)_2$ per second (Table I).

Table I. Yields and Molecular Weights Obtianed with $Cp_2Ti(Ph)_2$ at Different Aluminum Concentrations[a]

Ti, mmol	Al, mmol	C_3H_6, mol	yield, g	turnovers,[b] s^{-1}	$10^{-4}\bar{M}_n$	$\bar{M}_w/\bar{M}_n$
0.062	20.5	4.0	4.5	0.48	7.47	1.9
0.056	41.0	4.8	11.4	1.22	14.4	1.9
0.017	41.0	4.0	3.4	1.35	17.6	1.6
0.061	61.5	4.0	17.6	1.92	16.7	1.7
0.066	164	5.4	34.5	3.43	27.1	1.7
0.065	164	4.3	39.5	4.47	30.7	1.6

[a] Polymerization conditions: 400 cm^3 of toluene, −60 °C, 1 h. These polymerizations were initiated by adding propylene. All others by injection of the catalyst. [b] Rate in moles of propylene/mole of Ti/s.

The propagation kinetics at low Ti concentrations and practical Al levels are consistent with low conversions to species **2** and **3** in Scheme I.

Under pseudo-first-order conditions:

$$\text{rate} = k_{obsd}[C_3H_6][C][Ti] \quad (1)$$

with

$$k_{obsd} = k_p K_c K_m/(1 + K_m[C_3H_6] + K_c[C]) \quad (2)$$

and

$$K_m[C_3H_6] + K_c[C] \ll 1 \quad (3)$$

Scheme I is analogous to the modern mechanism postulated for ethylene polymerizations with titanocene derivatives and $AlC_2H_5Cl_2$.[14] Species **1** and **4** represent coordinatively unsaturated Ti(IV) complexes which are formally d^0 16-electron pseudotetrahedral species. Species **3** has the monomer coordinated at an a_1 molecular orbital. The three noncyclopentadienyl ligands

(16) Erker, G.; Berg, K.; Treschanke, L. *Inorg. Chem.* **1982**, *21*, 1277–1278.

(17) (a) Summers, L.; Uloth, R. H. *J. Am. Chem. Soc.* **1954**, *76*, 2278. (b) Wild, F. R. W. P.; Zsolnai, L.; Huttner, G.; Brintzinger, H. H. *J. Organomet. Chem.* **1982**, *232*, 233–247.

(18) (a) Stehling, F. C.; Knox, J. R. *Macromolecules* **1975**, *8*, 595. (b) Zambelli, A.; Locatelli, P.; Bajo, G.; Bovey, F. A. *Macromolecules* **1975**, *8*, 687.

(19) Zambelli, A.; Locatelli, P.; Zannoni, G.; Bovey, F. A. *Macromolecules* **1978**, *11*, 923–924.

Table II. Yields and Molecular Weights of Polypropylenes Obtained with the $Cp_2Ti(Ph)_2$/Methylalumoxane System at Different Temperatures[a]

T, °C	Ti, mM	Al, mM	C_3H_6, M	time, h	yield, g	$10^{-4}\bar{M}_n$	$\bar{M}_w/\bar{M}_n$	[N],[b] mol/mol of Ti
50	0.0361	18	10.7	0.50	1.7	0.315	*c*	34
25	0.125	23	4.98	0.50	1.0	0.212	*c*	5.2
0	0.131	24	5.23	0.50	3.4	0.390	*c*	6.3
−15	0.135	24	5.38	0.50	2.7	0.972	1.8	3.1
−30	0.139	25	5.54	0.50	10.2	3.67	1.7	3.1
−45	0.142	26	5.69	0.50	13.0	7.30	1.6	2.0
−60	0.149	26	5.93	0.50	4.0	5.52	1.7	0.80
−75	0.150	27	6.00	0.50	1.4	2.85	1.5	0.33
−85	0.152	28	6.11	1.92	1.4	3.38	1.6	0.46

[a] 400 cm³ of toluene. [b] Number of polymer molecules per titanium atom. [c] M_n by NMR.

Table III. Yields and Molecular Weights of Polypropylenes Obtained with the $Cp_2Ti(Ph)_2$/Methylalumoxane System at Different Temperatures and Times[a]

T, °C	Ti,[b] mM	Al, mM	C_3H_6, M	time, min	yield, g	$10^{-4}\bar{M}_n$	$\bar{M}_w/\bar{M}_n$	[N], mol/mol of Ti
−30	0.139	25	5.54	5	3.7	3.61	1.5	1.13
−30	0.139	25	5.54	10	4.1	3.25	1.7	1.40
−30	0.139	25	5.54	30	10.2	3.67	1.7	3.07
−30	0.139	25	5.54	60	11.1	2.88	1.7	4.26
−30	0.139	25	5.54	120	19.7	3.40	1.7	6.41
−30	0.139	25	5.54	180	25.5	3.05	1.8	9.25
−60	0.146	26	5.84	5	0.50	2.24	1.2	0.25
−60	0.146	26	5.84	10	1.00	3.27	1.3	0.34
−60	0.146	26	5.84	30	4.00	5.52	1.7	0.80
−60	0.146	26	5.84	60	5.9	7.08	1.6	0.92
−60	0.146	26	5.84	90	8.6	11.9	1.6	0.80
−60	0.146	26	5.84	120	9.4	9.31	1.7	1.12
−60	0.146	26	5.84	180	13.9	12.5	1.7	1.23
−60	0.146	26	5.84	240	27.3	18.6	1.7	1.62
−60	0.146	26	5.84	360	40.1	19.5	1.8	2.28
−75	0.15	27	6.00	5	0.50	2.16	1.5	0.15
−75[c]	0.15	27	6.00	10	0.80	2.44	1.9	0.22
−75	0.15	27	6.00	30	1.4	2.85	1.5	0.33
−75	0.15	27	6.00	120	4.10	4.60	1.5	0.59
−75	0.15	27	6.00	180	6.90	6.14	1.6	0.75

[a] 400 cm³ of toluene [b] Millimolar concentrations. [c] Asymmetrical GPC.

occupy a common equatorial plane with the growing chain held between two lateral coordination sites accommodating an unidentified noncyclopentadienyl anion and the monomer.

The specific mode of catalyst/cocatalyst interaction in species **2** (Scheme I) and the nature of the second noncyclopentadienyl ligand anion (R′) have not yet been identified. The bimetallic species are assumed to be outer-sphere complexes for the purposes of this discussion.

Polymerization rates and molecular weights are found to be a maximum at −45 °C (Table II). This is a consequence of catalyst instability above −45 °C. A plot of $1/R_p$ vs. time at −30 °C is linear, suggesting deactivation is second order in Ti. Catalyst deactivation with reduction to Ti(III) at −30 °C and at the concentrations in Table III was observed to occur with a catalyst half-life of about 1 h.

Typical polymerization rates and polymer molecular weights as a function of time are summarized in Table III and plotted according to eq 4 in Figure 2. [C*] represents the fraction of

$$[N] = [C^*] + k_{tr}[C^*]t \quad (4)$$

Ti present as active propagation centers, k_{tr} is the sum of pseudo-first-order rate constants for chain transfer, and [N] represents the number of polymer chains produced per Ti center with the assumption of one chain per active site.[20] The mean chain lifetimes ($1/k_{tr}$) increase from approximately 30 min at −30 °C to 80 min at −60 °C. [C*] decreases from 1 to 0.4 over the same temperature range.[21] Rates decrease with increasing time below

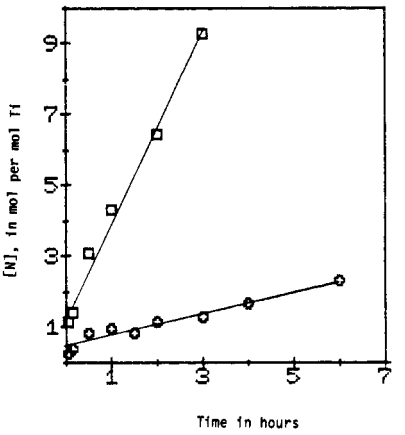

Figure 2. Linear relationship between polymerization time and number of polymer chains per titanium atom, [N]: (□) at −30 °C; (○) at −60 °C.

−60 °C due to catalyst precipitation. The concentrations of active sites with this soluble system are one to two orders of magnitude higher than those reported for heterogeneous Ti(III) polypropylene catalysts.[20,21]

Propylene Microstructures Obtained with $Cp_2Ti(Ph)_2$. Propylene polymerizations with group 4B bis(cyclopentadienyl)M(IV) derivatives (M = Ti or Zr) and methylalumoxane cocatalysts have yielded only atactic stereosequenes in the past.[12,13] An example of the ^{13}C NMR spectrum of the methyl pentad region of atactic polypropylene obtained with a zirconium-based catalyst system is shown in Figure 3. The NMR bands have been previously assigned to the ten unique steric arrangements of five adjacent monomer units:[10,18,19]

(20) Doi, Y.; Morinago, A.; Keii, T. *Macromol. Chem., Rapid Commun.* **1980**, *1*, 193–196.

(21) Equation 4 predicts anomalously high [C*] under conditions where the the catalysts are unstable: Cooper, W. In "Comprehensive Chemical Kinetics"; Bamford, C. H., Ed.; Elservier: Amsterdam, 1976; Vol. 15, pp 249–257.

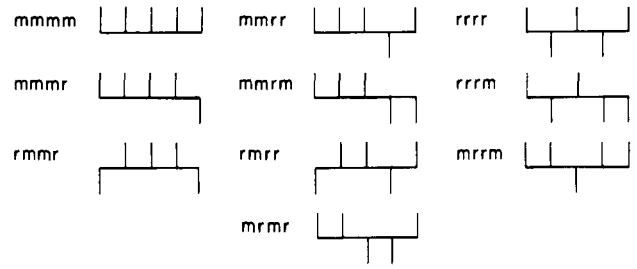

Only nine bands are observed with pentad resolution since the mmrm and rmrr pentads have the same chemical shift. The nine bands are divided into three distinct regions corresponding to mm-, mr-, and rr-centered pentads. The sums of the intensities of the three bands in each region correspond to the mm, mr, and rr triads. The fraction of meso placements (m dyads) is the sum of the mm and half the mr triads. A copolymerization scheme for the two prochiral faces of the monomer and the probability theory used for deriving the equations used in calculating the relative NMR band intensities are included as an Appendix.

Figure 4 shows the changes in intensity of the ^{13}C NMR spectra of the methyl pentad region of polypropylene obtained with the $Cp_2Ti(Ph)_2$/methylalumoxane system as the polymerization temperature changes from 25 to −45 °C. At 0 °C the rr-centered pentads (i.e., the rr triad) are greatly reduced in intensity. Finally, all the pentads are considerably depleted with the exception of the bands due to the longer isotactic sequences (mmmm) and those associated with the stereoblock junctures (mmmr and mmrm in a 1:1 ratio) which define the polymer structures as that depicted by the Fischer projection (II).

Analyses of the relative intensities of the methyl pentads are consistent with the chirality of the methine of the last inserted monomer unit providing stereochemical control during the polymerization. The measured and calculated pentad intensities (Table V) are summarized as a function of temperature. The theoretical Bernoullian statistical equations for chain-end controlled stereospecific polymerizations listed in Table VI provide an excellent fit to the experimental intensities. The statistical fit shows that steric inversions during propagation by a chain-end control mechanism result in the new absolute configuration of the last inserted monomer unit becoming the most probable one in succeeding enchainments.

Polymer Microstructures Obtained with *meso*- and *rac*-Et-[Ind]$_2$TiCl$_2$. Stereorigid and chemically stable ethylene-bridged chiral *rac*-Et[Ind]$_2$TiCl$_2$ and the achiral stereoisomer *meso*-Et-[Ind]$_2$TiCl$_2$ were synthesized and tested as polymerization catalysts together. The relative intensities of the methyl steric triads for the polypropylene obtained with a mixture containing 56% chiral *rac*-Et[Ind]$_2$TiCl$_2$ and 44% achiral *meso*-Et[Ind]$_2$TiCl$_2$ at −60 °C are given in Table VII. The triad analysis is consistent with the polymer being a mixture of isotactic polypropylene with structure I (63%) and atactic polypropylene (37%). In addition, the polypropylene molecular weight distribution is in accord with the complexes remaining homogeneous during the polymerization.

A crystalline fraction of the polymer mixture (94 °C melting point) was collected by stirring the mixture in pentane at 25 °C and filtration with a fine porosity sintered glass filter. The spectra of the pentane-insoluble fraction and the filtrate are given in Figure 5. Results of the triad intensity analyses and triad mechanistic model tests on these spectra are summarized in Table VII, and a comparison of the experimental and theoretical pentad intensities of the spectrum of the filtrate is given in Table VIII.

Inspection of the data in Table VII shows that the molecular weights for the original sample and the filtrate are closely equivalent. The NMR-determined ratio of the two types of polymers is also roughly the same as the ratio of the meso- and rac-Ti stereoisomers during polymerization. These observations indicate the rac- and meso-Ti stereoisomers have similar propagation and termination rate constants. The rac stereoisomer is apparently only marginally more active.

PENTAD	SHIFT, ppm	BAND INTENSITIES EXPERIMENTAL	CALCULATED
mmmm	0.000	0.06	0.06
mmmr	0.248	0.11	0.12
rmmr	0.469	0.07	0.06
mmrr	0.771	0.11	0.12
mmrm / rmrr	0.971	0.30	0.12 / 0.12 = 0.25
mrmr	1.170	0.12	0.12
rrrr	1.462	0.06	0.06
rrrm	1.659	0.11	0.12
mrrm	1.843	0.06	0.06
		1.00	1.0

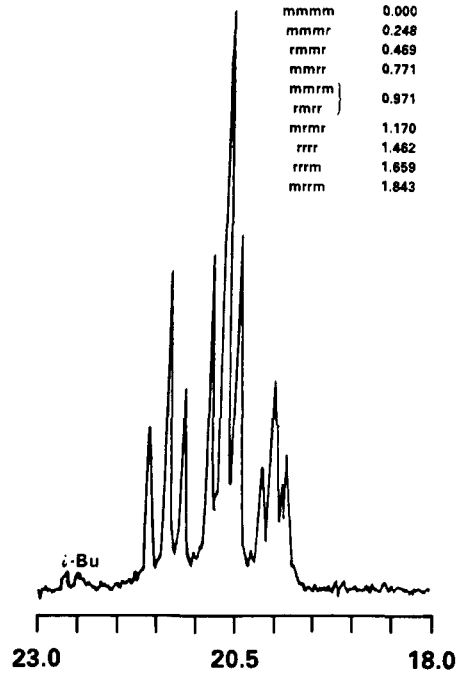

Figure 3. ^{13}C NMR spectra of the methyl pentad region for atactic polypropylene produced by $(Me_5Cp)(Cp)ZrCl_2$ at −30 °C.

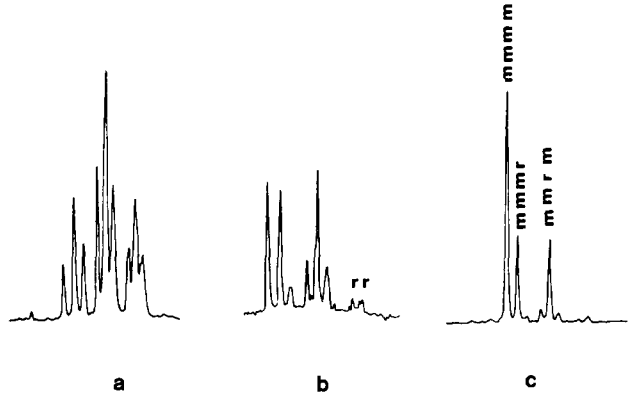

Figure 4. Comparison of ^{13}C NMR spectra of the methyl pentad region for polypropylene obtained with $Cp_2Ti(Ph)_2$/methylalumoxanes at three different polymerization temperatures: (a) 25 °C; (b) 0 °C; (c) −45 °C.

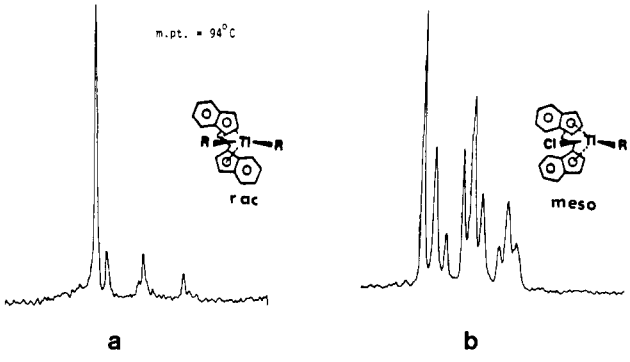

Figure 5. ^{13}C NMR spectra of the methyl pentad region of polypropylene obtained with stereoisomers of Et[Ind]$_2$TiCl$_2$ at −60 °C. (a) Pentane-insoluble fraction (25 °C). (b) Filtrate subsequent to removing part of the pentane-insoluble fraction.

The methyl pentad bands of the pentane-insoluble fraction were inadequately resolved for satisfactory analysis. However, triad intensity analyses and the triad mechanistic model tests on the spectrum of this fraction (Table VII) are in accord with the

Table IV. Dyad Compositions, Trid Fractions, and Triad Mechanistic Model Tests of ^{13}C NMR Spectra of the Methyl Region for Polypropylenes Obtained with $Cp_2Ti(Ph)_2$[a]

	stereoregularity						
	dyad comp		triad fractions			triad tests[b]	
polym temp. °C	[m]	[r]	[mm]	[mr+rm]	[rr]	$4[mm][rr_2]/[mr]^2$	2[rr]/mr
50	0.49	0.50	0.23	0.53	0.24	0.8	0.9
25	0.50	0.50	0.24	0.51	0.24	1.0	1.0
0	0.67	0.33	0.45	0.44	0.11	1.1	0.53
−15	0.78	0.22	0.62	0.33	0.05	1.1	0.30
−30	0.83	0.17	0.69	0.28	0.03	1.1	0.21
−45	0.85	0.15	0.73	0.25	0.02	1.1	0.16
−60	0.85	0.15	0.73	0.24	0.03	1.4	0.25
−75	0.85	0.15	0.72	0.25	0.02	1.1	0.18
−85	0.84	0.16	0.72	0.25	0.03	1.2	0.22

[a] Steroregularity independent of time and reactant concentrations. [b] $4[mm][rr]/[mr]^2 = 4IS/H^2 = 1$ for chain-end control; $2[rr]/[mr] = 2S/H = 1$ for site control

Table V. Calculated and Measured Steric Pentad Distributions of Polypropylenes Obtained with the $Cp_2Ti(Ph)_2$/Methylalumoxane System at Different Temperatures[a]

T, °C	% − m	mmmm	mmmr	rmmr	mmrr	mrmm + rmrr	rmrm	rrrr	rrrm	mrrm
50	50	0.06	0.13	0.06	0.13	0.25	0.13	0.06	0.13	0.06
		(0.06)	(0.13)	(0.06)	(0.13)	(0.25)	(0.13)	(0.06)	(0.13)	(0.06)
25	50	0.05	0.12	0.07	0.11	0.26	0.14	0.06	0.11	0.08
		(0.06)	(0.13)	(0.06)	(0.125)	(0.25)	(0.125)	(0.06)	(0.13)	(0.06)
0	67	(0.20)	0.19	0.06	0.08	0.26	0.09	0.01	0.05	0.06
		(0.20)	(0.20)	(0.05)	(0.10)	(0.25)	(0.10)	(0.01)	(0.05)	(0.05)
−15	78	0.34	0.23	0.05	0.05	0.22	0.06	0.004	0.02	0.03
		(0.38)	(0.21)	(0.03)	(0.06)	(0.22)	(0.06)	(0.002)	(0.02)	(0.03)
−30	83	0.46	0.19	0.03	0.06	0.18	0.05	0.001	0.008	0.014
		(0.48)	(0.19)	(0.02)	(0.04)	(0.19)	(0.05)	(0.001)	(0.007)	(0.020)
−45	85	0.52	0.20	0.01	0.04	0.18	0.03	0.001	0.008	0.013
		(0.53)	(0.18)	(0.02)	(0.03)	(0.19)	(0.03)	(0.0005)	(0.005)	(0.016)
−60	85	0.53	0.17	0.03	0.05	0.17	0.03	0.004	0.007	0.017
		(0.52)	(0.18)	(0.02)	(0.03)	(0.19)	(0.03)	(0.0005)	(0.006)	(0.016)
−75	85	0.50	0.19	0.02	0.04	0.19	0.03	0.004	0.011	0.019
		(0.49)	(0.19)	(0.02)	(0.04)	(0.20)	(0.04)	(0.001)	(0.01)	(0.018)
−85	84	0.51	0.18	0.02	0.04	0.18	0.03	0.002	0.008	0.018
		(0.51)	(0.19)	(0.02)	(0.03)	(0.19)	(0.03)	(0.001)	(0.006)	(0.017)

[a] Theoretical intensities in parentheses from the Bernoullian equations in Table VI.

Table VI. Stereochemical Sequence Designations and Probabilities for Dyads, Triads, and Pentads for Bernoullian and Enantiomorphic-Site Control Models (One Adjustable Parameter)

C type	Bernoullian[a]		enatiomorphic site[b]	
m	P		$1 - 2\beta(1 - \beta)$	
r	$(1 - P)$		$2\beta(1 - \beta)$	
mm	P^2		$1 - 3\beta(1 - \beta)$	
mr	$2P(1 - P)$	$4[mm][rr]/[mr]^2 = 1$	$2\beta(1 - \beta)$	$2[rr]/[mr] = 1$
rr	$(1 - P)^2$		$\beta(1 - \beta)$	
mmmm	P^4		$5\beta^4 - 10\beta^3 + 10\beta^2 - 5\beta + 1$	
mmmr	$2P^3(1 - P)$		$-6\beta^4 + 12\beta^3 - 8\beta^2 + 2\beta$	
rmmr	$2P^2(1 - P)^2$		$\beta^4 - 2\beta^3 + \beta^2$	
mmrr	$2P^3(1 - P)$		$-6\beta^4 + 12\beta^3 - 8\beta^2 + 2\beta$	
mrmm + rmrr	$P^2(1 - P)^2$	mmmr:mmrm = 1:1	$2\beta^4 - 4\beta^3 + 2\beta^2$	mmmr:mmrr:mrrm 2:2:1
rmrr	$2P(1 - P)^3$		$2\beta^4 - 4\beta^3 + 2\beta^2$	
rmrm	$2P^2(1 - P)^2$		$2\beta^4 - 4\beta^3 + 2\beta^2$	
rrrr	$2P(1 - P)^3$		$\beta^4 - 2\beta^3 + \beta^2$	
rrrm	$P^2(1 - P)^2$		$2\beta^4 - 4\beta^3 + 2\beta^2$	
mrrm	$(1 - P)^4$		$-3\beta^4 + 6\beta^3 - 4\beta^2 + \beta$	

[a] Reference 11. [b] References 6 and 9.

polymer having an isotactic microstructure produced according to the enantiomorphic-site control model with a probability parameter $\beta = 0.89$.

The relative pentad band intensities of the filtrate (Table VIII) are consistent with the equations (Table IX) applicable to either a mixture of polmers produced by two species with one species producing atactic polymer (weight fraction = 0.72) and the other obeying the enantiomorphic-site model ($\beta = 0.89$) or an isotactic–atactic block polymer resulting from Al-catalyzed meso/rac isomerizations of Ti. The good fit of the pentad intensity data to these equations proves that the isotactic portion of the polymer was obtained with a catalyst following the enantiomorphic-site control mechanism and that it has structure I. The catalyst chirality dictates the stereoregulation in this mechanism resulting in the occasional steric inversions in the chain being predominantly reversed in succeeding monomer enchainments.

Stereochemistry of Double Bond Addition. Diisotactic polypropylene (PPd_5) with the novel stereoblock structure (Scheme II) was prepared from *cis*-CD_3CD_2=CHD to determine if cis or trans addition occurs during the polymerizations leading to

Table VII. Dyad Compositions, Triad Fractions, and Mechanistic Model Tests of ^{13}C NMR of the Methyl Pentad Region for Polypropylenes Made with Soluble Stereoisomers of $Et[Ind]_2TiCl_2$/Methylalumoxane Systems

			stereoregularity							
	polymer[a]			dyad comp		triad fractions			triad tests	
	$10^{-4}\bar{M}_n$	$10^{-4}\bar{M}_w$	param-eters[b]	[m]	[r]	[mm]	[mr + rm]	[rr]	4[mm][rr]/[mr]^2	2[rr]/[mr]
product	9.66	15.4	$\beta = 0.89$ $w_1 = 0.37$	0.69 (0.69)	0.31 (0.30)	0.54 (0.54)	0.30 (0.31)	0.16 (0.15)	3.3	1.1
"soluble" filtrate[c]	8.76	14.7	$\beta = 0.89$ $w_1 = 0.72$	0.59 (0.58)	0.41 (0.42)	0.38 (0.38)	0.42 (0.41)	0.21 (0.21)	1.8	1.0
insoluble fraction[d]			$\beta = 0.89$ $w_1 = 0.0$	0.80 (0.80)	0.20 (0.20)	0.71 (0.71)	0.19 (0.20)	0.10 (0.10)	5.3	1.0

[a] Polymerization conditions: −60 °C, 0.086 mmol of $Et[Ind]_2TiCl_2$ (56% rac and 44% meso mixture of stereoisomers by ^1H NMR intensity ratios of the complexes), 9.4 mmol of Al, 2.4 mol of C_3H_6, 400 cm^3 of toluene, 4.25 h. Yield = 6.4 g. [b] Theoretical NMR intensities in parentheses calculated from the equations in Table IX. [c] Remaining fraction of polymer following removal of a part or all of the pentane-insoluble portion at 25 °C. [d] Pentane-insoluble fraction at 25 °C.

Table VIII. Comparison of Calculated and Experimental Band Intensities for the Filtrate of Sample Obtained with *rac*- + *meso*-$Et[Ind]_2TiCl_2$[a]

	band intensities		
pentad	exptl	calcd	diff
mmmm	0.18	0.20	−0.02
mmmr	0.14	0.13	0.01
rmmr	0.06	0.05	0.01
mmrr	0.11	0.13	−0.02
mrmm + rmrr	0.20	0.19	0.01
rmrm	0.11	0.10	0.01
rrr	0.04	0.05	−0.01
rrrm	0.11	0.10	0.01
mrrm	0.06	0.06	0.00

[a] Sample following removal of either part of or all of the pentane-insoluble fraction at 25 °C. Equations in Table IX. Parameters are $\beta = 0.89$ and $w_1 = 0.72$.

Table IX. Relative Band Intensities for Atactic–Isotactic Block Polymers or a Mixture of Two Polymers Obtained from a Mixture of a Site Controlled Species and a Species Having No Stereochemical Control[a]

C type	intensities
m	$0.5w_1 + (1 - w_1)[1 - 2\beta(1 - \beta)]$
r	$0.5w_1 + (1 - w_1)[2\beta(1 - \beta)]$
mm	$0.25w_1 + (1 - w_1)[1 - 3\beta(1 - \beta)]$
mr	$0.5w_1 + (1 - w_1)[2\beta(1 - \beta)]$
rr	$0.25w_1 + (1 - w_1)[\beta(1 - \beta)]$
mmmm	$0.0625w_1 + (1 - w_1)[5\beta^4 - 10\beta^3 + 10\beta^2 - 5\beta + 1]$
mmmr	$0.125w_1 + (1 - w_1)[-6\beta^4 + 12\beta^3 - 8\beta^2 + 2\beta]$
rmmr	$0.0625w_1 + (1 - w_1)[\beta^4 - 2\beta^3 + \beta^2]$
mmrr	$0.125w_1 + (1 - w_1)[-6\beta^4 + 12\beta^3 - 8\beta^2 + 2\beta]$
mrmm	$0.125w_1 + (1 - w_1)[2\beta^4 - 4\beta^3 + 2\beta^2]$
rmrr	$0.125w_1 + (1 - w_1)[2\beta^4 - 4\beta^3 + 2\beta^2]$
rmrm	$0.125w_1 + (1 - w_1)[2\beta^4 - 4\beta^3 + 2\beta^2]$
rrrr	$0.0625w_1 + (1 - w_1)[\beta^4 - 2\beta^3 + \beta^2]$
rrrm	$0.125w_1 + (1 - w_1)[2\beta^4 - 4\beta^3 + 2\beta^2]$
mrrm	$0.0625w_1 + (1 - w_1)[-3\beta^4 + 6\beta^3 - 4\beta^2 + \beta]$

[a] w_1 = weight fraction of atactic polymer. Mixture satisfies the triad test (2S/H = 1.0) and pentad 2:2:1 condition for mmr:mmrr:mrrm intensities for site control material.

structure II. The ^1H NMR spectrum of the product showing the bands corresponding to the various steric tetrads of the methylene CH groups in the polymer is shown in Figure 6. Band assignments were taken from the literature,[18a] with the exception of the mrm tetrad which is shown to be coincident with the rrr tetrad from the band intensities found in this work.

The intensity of the shaded R_3C-H band at about 1.5 ppm is consistent with a significant concentration of isotopic impurities in the monomer feed. (End-group analyses (vide infra) show that this signal does not arise from hydrolysis of coordination methines.) The peaks shaded between 0.84 to 0.75 ppm are ascribed to isotopic impurities at the methyl and methylene carbons and to chain-end methyl groups of low molecular weight material re-

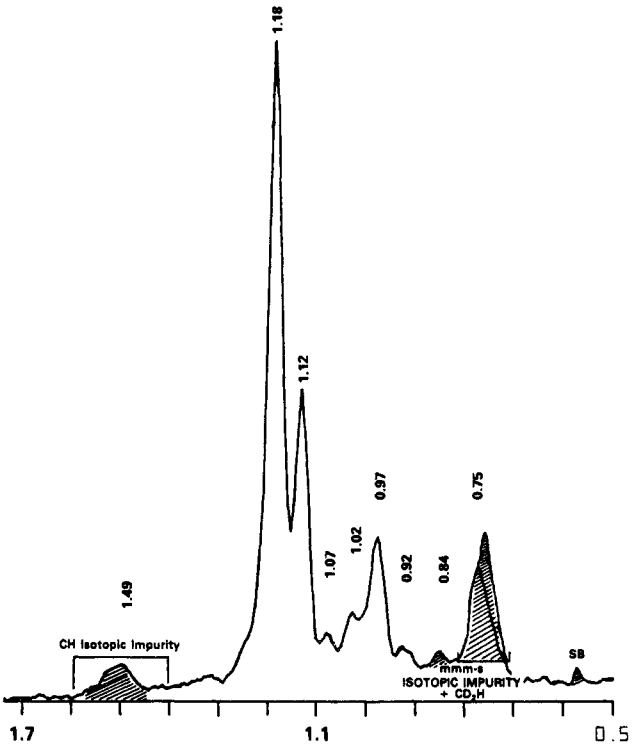

Figure 6. ^1H NMR spectrum of diisotactic stereoblock polypropylene made from *cis*-CD_3CD_2=CHD with $Cp_2Ti(Ph)_2$/methylalumoxane at about −60 °C.

Scheme II. Stereochemistry of Double Bond Addition with *cis*-CD_3CD=CDH

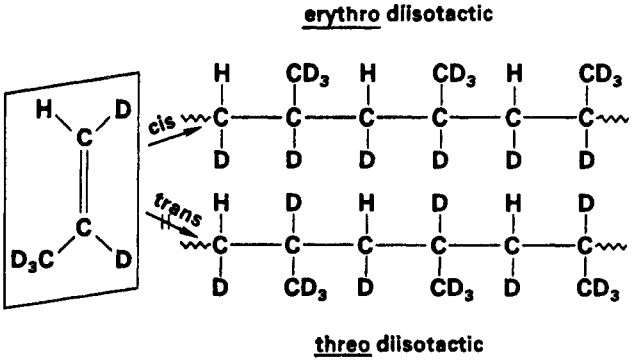

Table X. Stereochemical Sequence Designation and Bernoullian Probabilities for Tetrads

tetrad	projection	bernoullian probability
mmm		P^3
mmr		$2P^2(1-P)$
rmr		$P(1-P)^2$
mrm		$P^2(1-P)$
rrm		$2P(1-P)^2$
rrr		$(1-P)^3$

mmr, rmr, mrm: 2:1

Table XI. Experimental vs. Calculated Intensities for PPd_5[a]

H type	chemical shift, ppm	exptl intensity	calcd intensity for Bernoullian chain	diff
mmm-a	0	0.44	0.47	−0.03
mmr-a	0.06	0.27	0.27	0.00
rmr-a	0.11	0.06	0.04	+0.02
rrm-1	0.16	0.04	0.04	0.00
mrm[b]	0.21	0.15	0.13	+0.01
rrr			0.01 (−0.14)	
rrm-2	0.26	0.04	0.04	0.00

[a] PPd_5 made from *cis*-CD_3CD=CHD between −60 and −30 °C with 20 cm³ of a 1 M Al stock toluene solution, 100 mg of $Cp_2Ti(Ph)_2$ in 5 cm³ of toluene, and about 2 g of monomer (78% − m). [b] mrm tetrad assigned from these intensity calculations. [c] mmr-s and [mmm-s + -CD_2H] terminal groups at 0.34 and 0.43 ppm, respectively.

sulting from the high catalyst concentration and low monomer concentration employed.

The tetrad bands arise from *anti*-methylene protons and not from the corresponding *syn*-methylene protons. This proves an erythro-diisotactic structure which is consistent with insertion occurring through cis addition to the double bond with retention of configuration at the coordination carbon (Scheme II).

Table X contains the stereochemical designations of all the possible tetrads for the methylene protons in the polymer and their intensity ratios for an end-group control model. The experimental and calculated intensities using the Bernoullian statistical model are shown in Table XI. Good agreement is found between the theoretical and experimental values. The H atoms are in an isotactic-stereoblock environment with respect to each other with roughly the same degree of stereoregularity as measured for the methyl pentad region of polymers made from $CH_3CH{=}CH_2$ under similar conditions.

Regiospecificity. ^{13}C NMR analyses of the end groups of the polymer chains have indicated that the methylene carbon atom of the last inserted monomer is bound to the transition metal during chain initiation and termination, i.e., position 1 according to IUPAC nomenclature.[15] The polypropylene end-group analyses summarized in Table XII are in accord with this conclusion.

$$\underset{(1)}{CH_2}{=}\underset{(2)}{CHR}$$

Polymerizations under the same conditions with either Zr or Ti metallocene based catalysts gave polypropylenes with very similar end-group analyses.

An approximate 1:1 ratio of *n*-propyl:vinyl chain ends at 50 °C (Table XII) is consistent with "1–2" initiation involving the β-hydrogen of a previously existing chain for most of the polymer. Aspecific "1–2" initiation by methyl groups and terminations with transfer to Al are implied by the exclusive occurrence of isobutyl end groups at sufficiently low temperatures.

Head-to-head (H–H) and tail-to-tail (T–T) enchainments in the higher molecular weight polymers were sufficiently low as to be undetectable by NMR. Indeed, stereoirregularities from

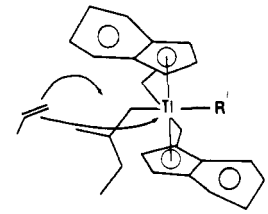

Figure 7. Alternative lateral and central monomer coordination sites available to *rac*-Et[Ind]$_2$TiCl$_2$.

Scheme III

$$Ti{\vdash}\cdots + C_3H_6 \xrightarrow{k_{1,1}} Ti{\vdash}{\vdash}\cdots \quad (H\text{-}T) \quad "1\text{-}2" \quad (1)$$

$$Ti{\vdash}\cdots + C_3H_6 \xrightarrow{k_{1,2}} Ti{\dashv}{\vdash}\cdots \quad (T\text{-}T) \quad "2\text{-}1" \quad (2)$$

$$Ti{\dashv}\cdots + C_3H_6 \xrightarrow{k_{2,1}} Ti{\vdash}{\dashv}\cdots \quad (H\text{-}H) \quad "1\text{-}2" \quad (3)$$

$$Ti{\dashv}\cdots + C_3H_6 \xrightarrow{k_{2,1}} Ti{\dashv}{\dashv}\cdots \quad (H\text{-}T) \quad "2\text{-}1" \quad (4)$$

secondary insertions were sufficiently infrequent for the stereochemical sequence of the polymer configurations to be completely accounted for by statistical models which assume complete regiospecificity.

It can be concluded that the propylene enchainments are typical for Ti-based catalysts. They are primarily of a "1–2" type (C_1 to the catalyst, C_2 to the chain, preceding diagram) with $k_{1,1}$ being much greater than the other rate constants shown in the copolymerization scheme for regioselectivity (Scheme III).

Discussion

Bimetallic Species. The much faster rates and improved catalyst stabilities obtained with methylalumoxanes relative to simpler cocatalysts such as $AlC_2H_5Cl_2$ have not been accounted for.[12] Definitive structural characterization of the intermediates during catalysis may help resolve this issue in the future.

An inner-sphere hexacoordinate intermediate with an alumoxane oxygen coordinated to the transition metal and with the Al simultaneously linked to an outer-sphere bonding interaction with the Cp ligands has been speculated on.[22] It is noted that this bifunctional cocatalysis requires concomitant Cp reorganization from a delocalized structure to either an allylene with the metal bound to the allyl portion[23] or to a monohapto structure if the 18-electron rule is to be obeyed with monomer coordination at the transition metal. If such rearrangements are important they would probably be very transitory since the ligand effects on the polymer microstructure indicate that the Cp anions remain attached to the transition metal during catalysis.

Cocatalyst coordination or bridging at the unidentified non-Cp anion site is most probably not essential since *meso*-Et[Ind]$_2$TiCl$_2$ is a good polymerization catalyst despite the fact that the sheltering ring substituent fused to the cyclopentadiene ligand results in this coordination position being inaccessible to sterically demanding ligands.[17]

Monomer Coordination. The structure shown for intermediate **3** in Scheme I was originally suggested on the basis of theoretical calculations which led to the modern mechanism for group 4B metallocene catalyst polymerizations.[14] A recent crystal structure[24] of a pentacoordinate group 4B metallocene derivative supports the basic geometry of species **3** with the three non-Cp ligands in a common plane. Either the growing chain[14] or the monomer[25] can occupy the central coordination position dependent on the linear combination of frontier orbitals in the contrasting hybridization schemes.

The site controlled stereospecificity with *rac*-Et[Ind]$_2$TiCl$_2$ is consistent with monomer coordination at the lateral site (Figure

(22) Kaminsky, W.; Miri, M.; Sinn, H.; and Woldt, R. *Makromol. Chem., Rapid Commun.* **1983**, *4*, 417–421.

(23) (a) Rerek, M. E.; Basolo, F. *Organometallics* **1983**, *2*, 372–376. (b) Rerek, M. E.; Liang-Nian, J.; Basolo, F. *J. Chem. Soc., Chem. Commun.* **1983**, 1208–1209.

(24) Silver, M. E.; Fay, R. C. *Organometallics* **1983**, *2*, 44–47.

Table XII. Chain-End Methyl Groups and Yields of Polypropylene Obtained with the Zirconium/Methylalumoxane Polymerization Systems[a]

complex	T, °C	Zr, mmol	yield, g	$\bar{M}_n$[b]	% vinylidene[c]	% n-propyl[d]	% isopropyl[e]
Cp_2ZrCl_2	50	0.069	61	600	50	50	
$Me_5CpCpZrCl_2$	50	0.055	36	1420	40	40	20
$Me_5CpCpZrCl_2$	−30	0.143	2.7	7060			100

[a] Polymerization conditions: 41 mmol of Al; 0.45 dm^3 of toluene; 0.30 dm^3 of propylene; 2 h. [b] Estimated from NMR. [c] 22.5 ppm. [d] 14.6 ppm. [e] Two doublets of equal intensities at 23.4, 23.2, 22.6, and 22.4 ppm.[28] Atactic Polymers.

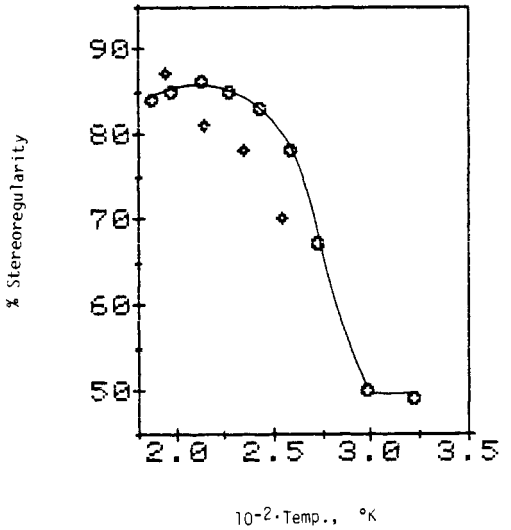

Figure 8. Temperature dependencies of stereoregularities for isotactic polypropylene (% − m) obtained with the $Cp_2Ti(Ph)_2$/methylalumoxane system (line) and syndiotactic polypropylene obtained with the VCl_4/$Al(C_2H_5)_2Cl$ system.

7). Models suggest that the methyl group of the coordinated monomer and the overhead ring fused to the cyclopentadiene ligand experience nonbonding contacts with lateral site coordination for only one face of the prochiral monomer. Similar interactions are not immediately apparent for monomer coordination at the alternative central coordination position.

The closely equivalent rates for *meso*- and *rac*-$Et[Ind]_2TiCl_2$ complexes are consistent with the former compound having two faces of the monomer available to one lateral coordination vacancy while, in principle, the latter species has one monomer face predominantly available to two lateral coordination positions.

Exclusive coordination of the monomer at the lateral site is, of course, questionable. The changes in stereospecificity for $Cp_2Ti(Ph)_2$ with temperature are consistent with changes in the relative importance of the position of monomer coordination at two alternative sites. The stereospecificity increases between 25 and −30 °C (Table IV) as the polymer chains gain the prerequisite conformational stability. The relative insensitivity of catalyst stereospecificity between −30 and −85 °C could imply monomer coordination at a less stereospecific site as the temperature decreases. Alternatively, the data may reflect the temperature dependencies of equilibria between contact and solvent-separated $[Cp_2TiR]^+/S/[Al]^-$ ion pairs.[34]

Chain-End Control. The $VCl_4/Al(C_2H_5)_2Cl$ syndiotactic-specific system[19] exhibits a similar degree of stereospecificity to the isotactic-specific $Cp_2Ti(Ph)_2$/methylalumoxanes catalyst system at equivalent temperatures (Figure 8). As is the case for the titanocene derivatives, the VCl_4-based system's stereospecificity is also governed by a chain-end control mechanism.[10]

The most significant differences in the mechanisms of polymerization with the two catalyst systems are in the regiospecificity of insertion. The soluble Ti isotactic-specific polymerization is consistent with a "1–2" cis-insertion mechanism with retention of configuration at the coordinated carbon while syndiotactic-specific Ziegler–Natta polymerizations conform to a "2–1" insertion mechanism.[10,26,27] This difference can be steric or electronic in origin. It is noted that the direction of polarization of the metal–carbon bond for V may differ as these species are unreactive toward methanol.[13]

Scheme IV. Mechanism of Stereoregulation for both Syndiotactic and Isotactic Chain-End Controlled Propylene Polymerizations

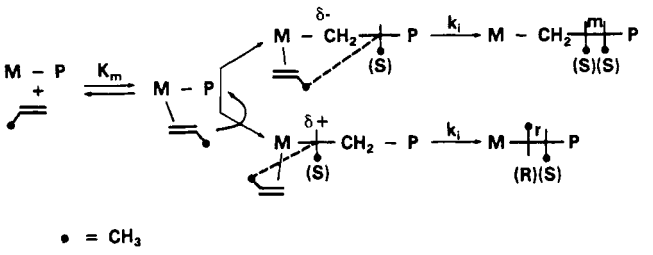

For both polymerization systems, the last inserted methine carbon with any particular absolute configuration (*R* or *S*) promotes enchainment of the same prochiral face of the incoming monomer (Si or Re, respectively) through basically similar steric interactions. As shown in Scheme IV a syndiotactic or isotactic placement results from the mode of monomer enchainment ("2–1" vs. "1–2" insertions, respectively). "Errors" in stereoregulation arise from a competing "copolymerization" of the two prochiral olefin faces rather than from regioirregularities.

The dashed lines in Scheme IV suggests that the monomer methyl groups and the stereoregulating methine chain-end groups are in a similar environment with respect to each other in both isotactic-specified Ti(IV) and syndiotactic-specific V(III) chain-end controlled polymerization systems. This provides a qualitative rationale for the similarity in the degrees of stereospecificity (% m and % r) in both polymerization systems.

Approximately 2 kcal/mol is typical for a $\Delta\Delta G^{\ddagger}$ (eq 5) for chain-end controlled Ziegler–Natta polymerizations.[19] This is consistent with stereoregulation arising from the nonbonding interactions between the monomer methyl group and the methine carbon substituents of the last inserted monomer unit.

$$k_m/k_r = m/r = \exp(\Delta\Delta S^{\ddagger}/R - \Delta\Delta H^{\ddagger}/RT) \qquad (5)$$

Calculations based on V(III) active sites (crystal ionic radius = 0.74 Å) have implied that preferential coordination of the same prochiral face of the monomer (K_m, Scheme IV) is plausible for chain-end controlled mechanisms with "2–1" insertions but not for "1–2" insertions.[29]

Consistent with these calculations, isotactic polypropylenes with structure II and having essentially identical degrees of stereoregularity at equivalent polymerization temperatures are obtained with a number of different metallocene derivatives such as Cp_2VCl_2, Cp_2TiCl_2, $Cp_2Ti(Ph)_2$, $Cp_2Ti(C_6F_5)Cl$, and $Cp_2Ti{=}CH_2{\cdot}ClAl(CH_3)_2$ whereas no stereoregulation has been detected with zirconocene derivatives. The larger crystal ionic radius of Zr(IV) (0.79 Å relative to Ti(IV) and V(IV) which are 0.68 and 0.63 Å, respectively) may result in the absence of van der Waals' contacts required for chain-end control in 1–2 cis additions with the zirconocenes.

(25) (a) Brintzinger, H. H. *J. Organomet. Chem.* **1979**, *171*, 337. (b) Alcock, N. W. *J. Chem. Soc. A* **1967**, 2001.

(26) (a) Takgami, Y.; Suzuki, T.; Okazaki, T. *Bull. Chem. Soc. Jpn.* **1969**, *42*, 1060; **1969**, *42*, 848; **1970**, *43*, 1484. (b) Zambelli, A.; Natta, G.; Pasquon, I. *J. Polym. Sci., Part C* **1964**, *4*, 411.

(27) Zambelli, A.; Locatelli, P.; Sacchi. M. C.; Rigamonte, E. *Macromolecules* **1980**, *13*, 798–800.

(28) Seebach, D.; Prelog, V. *Angew. Chem., Int. Ed. Engl.* **1982**, *19*, 857.

(29) Zambelli, A.; Allegro, G. *Macromolecules* **1980**, *13*, 42.

The relative rates of enchainment of each prochiral face of the monomer unit determine the reaction stereospecificity. Since $k_p = K_m k_i$ (Scheme IV) then the relative magnitudes of K_m (monomer coordination) or k_i (insertion) for the prochiral faces of the monomer are viable alternatives for considering what determines the degree of stereospecificity. Precedent for insertion rates controlling reaction stereochemistry has been noted in one case of asymmetric hydrogenation but with $\Delta\Delta G^{\ddagger} = 4$ kcal/mol.[30] This contrasts with the 2 kcal/mol for the chain-end controlled polymerizations and is coincident with the 4 kcal/mol measured for heterogeneous $TiCl_3$ catalysts.[19]

The fundamental reason for the chain-end control mechanism being inoperative with *meso*-Et[Ind]$_2$TiCl$_2$ is not clear-cut since there are several nonnegligible differences between this complex and $Cp_2Ti(Ph)_2$. The Cp ring substituents are electron withdrawing and may influence the Ti–ligand bond lengths, one of the non-Cp anion sites is inaccessible to bulky ligands since it is sandwiched between the Cp ring substituents, and the ethylene bridge restricts Cp ring torsional mobility.

The diastereoselective additions in the two polymerizations are then 1–3 inductions with the relative topocities of the reactants specified in the 1k,u1 nomenclature[28] as follows:

$$\text{isotactic stereoblock:} \quad u1 \xrightarrow{1,3} 1 \tag{6}$$

$$\text{syndiotactic:} \quad u1 \xrightarrow{1,3} u \tag{7}$$

Alternative Mechanisms Giving Structure II. α hydrogens can form C–H–Ti "agostic" bridges which have been suggested to control the stereospecificity of Ziegler–Natta polymerizations.[31] Agostic effects provide a simple and interesting mechanism for inducing chain-end conformational stability.

Both this mechanism and the novel proposal of transition-metal carbene intermediates[32] are considered less likely than a cis insertion mechanism since approximately equivalent $\Delta\Delta G^{\ddagger}$ values are found for the chain-end controlled isotactic-specific and syndiotactic-specific polymerizations. In the theoretical cases of carbenes or agostic hydrogens equivalent stereoregulation is implicated for chiral centers either arising from or involving dissimilar mechanisms and methylene groups.

Stereoregulation mechanisms involving isomerizations of chiral titanium sites,[33] aluminum transportation of polymer chains between enantiomeric sites after a series of insertions,[34] and bimolecular exchanges of polymer chains between soluble enantiomeric Ti complexes would yield structure II. These mechanisms would even be consistent with the methyl pentad distributions reported here on the condition that the catalysts are perfectly stereoregulating while the polymer chain is bound at each particular chiral site. This condition is unlikely since polypropylenes obtained with even the more highly stereoregulating soluble chiral species and the much more stereorigid heterogeneous Ti(III) catalysts contain 5–20% and about 2% racemic dyads,[6] respectively.

More importantly, the above three mechanisms for structure II are kinetically distinguishable from the chain-end control mechanism at −60 °C. C_3H_6, Al, and Ti concentrations do not influence the fraction of meso placements in the polymer. The isomerization mechanism can be ruled out since increasing the propylene concentration from less than 1 to 5 M did not increase % – m although the polymerization rates had a first-order dependence on monomer. The mechanism invoking Al transportation of the polymer chains between enantiomorphic sites can be disregarded since increasing the Al concentration from 0.03 to 1 M did not decrease % – m. Similarly, bimolecular exchanges of polymer chains between enantiomorphic complexes can be discarded since increasing the Ti concentration from 0.15 to 12.5 mM did not decrease the polymer stereoregularity.

Concluding Remarks

The concentrations of active sites with this soluble catalyst system are between one and two orders of magnitude higher than those reported for heterogeneous Ti(III) polypropylene catalysts while the mean lifetimes of the chains are not exceptionally long.[21]

A new isotactic polypropylene microstructure has been obtained with a pentad distribution consistent with a chain-end stereoregulation mechanism. The stereoregulation process is analogous to known syndiotactic specific polymerizations with soluble vanadium catalysts. Isotactic and syndiotactic specific polymerizations are a consequence of "1–2" and "2–1" monomer enchainments, respectively.

Soluble catalysts with stereorigid chiral ligands have been shown to produce isotactic polypropylene with the same microstructure as that found for polymers obtained with heterogeneous catalysts. It is concluded that syndiotactic polypropylene can, in principle, be produced with an enantiomorphic-site control mechanism following a "2–1" mode of insertion. Indeed, these polymers would have pentad distributions analogous to site controlled isotactic polymers but with m and r reversed in the relative pentad intensity equations.

Finally, it is noted that the sensitivity of the polymer microstructures to structural features of the catalysts provides an unusual opportunity for inferences to be drawn regarding the structures of the reaction intermediates and the mechanisms of stereoregulation and polymerization. In this regard, evidence that both the chain-end and enantiomorphic-site stereoregulating mechanisms can be operative simultaneously will be the subject of a future publication.

Acknowledgment. I am indebeted to Dr. Eric Tornqvist and Dr. F. C. Stehling of our laboratories for valuable discussions which aided this study. It also thank C. U. DeGracia and C. K. Ruff for assistance in preparing polymer samples and obtaining NMR spectra, respectively.

Appendix

The origins of the parameters and the equations for the relative methyl pentad intensities of the polymers are pointed out in this section. *R* and *S* notations are used for the absolute configurations of the chain-end methine units during the chain lifetimes with the catalyst, represented by M, given highest priority and shown on the left.

stereoselective "coloymerization"	probability
$M\text{–}R\cdots + C_3H_6 \xrightarrow{k_{RR}} M\text{–}R\text{–}R\cdots$	$P_{RR} = k_{RR}/(k_{RR} + k_{RS})$ (1)
$M\text{–}R\cdots + C_3H_6 \xrightarrow{k_{RS}} M\text{–}S\text{–}R\cdots$	$P_{SR} = k_{RS}/(k_{RR} + k_{RS})\ (1 - P_{RR})$ (2)
$M\text{–}R\cdots + C_3H_6 \xrightarrow{k_{SS}} M\text{–}S\text{–}S\cdots$	$P_{SS} = k_{SS}/(k_{SS} + k_{SR})$ (3)
$M\text{–}R\cdots + C_3H_6 \xrightarrow{k_{SR}} M\text{–}S\text{–}S\cdots$	$P_{RS} = k_{SR}/(k_{SS} + k_{SR})\ (1 - P_{SS})$ (4)

Analogous copolymerization schemes apply for enantiomeric catalyst sites leading to predominantly *R*- or *S*-coordinated chain ends.

As for copolymerizations of two distinct monomer units,[35] the mole fraction of *R* units in the polymer chain (immediately after the last insertion and prior to termination) can be expressed in terms of the "reactivity ratios" in the "copolymerization" scheme

(30) Chan, A. S. C.; Pluth, J. J.; Halpern, J. *J. Am. Chem. Soc.* **1980**, *102*, 5952–5954.
(31) Brookhart, M.; Green, L. H. *J. Organomet. Chem.* **1983**, *250*, 395–408.
(32) Ivin, R. J.; Rooney, J. J.; Stewart, C. D.; Green, M. L. H.; Mahtab, R. J. *J. Chem. Soc., Chem. Commun.* **1978**, 604–606.
(33) (a) Langer, A. *Ann. N.Y. Acad. Sci.* **1977**, *295*, 100–126. (b) Kennedy, J. P.; Langer, A. W. *Fortschr. Hochpolym.-Forsch.* **1969**, *3*, 508–580.
(34) Natta, G.; Pasquon, I. *Adv. Catal.* **1959**, *11*, 30.
(35) (a) Alfrey, T.; Goldfinger, J. *J. Chem. Phys.* **1944**, *12*, 322. (b) Mayo, F. R.; Lewis, F. M. *J. Am. Chem. Soc.* **1944**, *66*, 1594.

for the Re and Si prochiral faces of the monomer.

$$F_R = \frac{r_1 + 1}{r_1 + r_2 + 2} \quad (5)$$

With [Re] = [Si], $r_1 = k_{RR}/k_{RS}$ and $r_2 = k_{SS}/k_{SR}$. Substitutions in eq 5 from eq 1-4 and rearrangement yields F_R in terms of the substitution probabilities:

$$F_R = (1 - P_{SS})/(2 - P_{SS} - P_{RR}) \quad (6)$$

Similarly,

$$F_S = (1 - P_{RR})/(2 - P_{SS} - P_{RR}) \quad (7)$$

As an example, the probability of an *RRRRR* stereosequence during chain growth at a particular catalyst site (a mmmm pentad) is obtained by substitution into eq 8

$$P_{RRRRR} = [F_R][P_{RR}][P_{RR}][P_{RR}][P_{RR}] \quad (8)$$

The sequence distributions of the polymers made at either enantiomeric site are identical. The total intensity of the mmmm pentad in the general case is obtained as the sum of *RRRRR* and *SSSSS* contributions produced by a particular site. To avoid an implication of chirality in polymer chains detached from the catalyst the parameters P_{RR}, F_R, P_{SS}, and F_S are relabeled P_a, F_a, P_b, and F_b, respectively

$$\text{mmmm} = F_a[P_a]^4 + F_b[P_b]^4 \quad (9)$$

The pentad equation simplifies to the chain-end control model when

$$k_{RR} = k_{SS} \quad (10)$$

and

$$k_{RS} = k_{SR} \quad (11)$$

Substituting from eq 10 and 11 into eq 1 and 3 results in

$$P_a = P_b = P \quad (12)$$

Substitution of P in eq 6 and 7 gives

$$F_a = F_b = 0.5 \quad (13)$$

Substitution into eq 9 from eq 12 and 13 gives

$$\text{mmmm} = P^4 \quad (14)$$

From the probability of a meso dyad

$$\text{m} = 0.5P + 0.5P = P \quad (15)$$

Atactic polymers have m = 0.5. The equations simplify to the enantiomorphc-site control model when, at each chiral site,

$$k_{SR} = k_{RR} \quad (16)$$

$$k_{RS} = k_{SS} \quad (17)$$

Substitution from eq 16 and 17 into eq 2 and 3 shows

$$P_{SS} = P_{SR} = (1 - P_{RR}) \quad (18)$$

Substitution from eq 18 into eq 6 yields

$$F_a = P_a = \beta \quad (19)$$

Similarly, eq 7 gives

$$F_b = (1 - P_a) = P_b = (1 - \beta) \quad (20)$$

Substituting from eq 19 and 20 into eq 9

$$\text{mmmm} = \beta^5 + (1 - \beta)^5 \quad (21)$$

or

$$\text{mmmm} = 5\beta^4 - 10\beta^3 + 10\beta^2 - 5\beta + 1 \quad (22)$$

The equations for the other pentads for each mechanism can be obtained similarly.

Registry No. $Cp_2Ti(Ph)_2$, 1273-09-2; *meso*-Et[Ind]$_2TiCl_2$, 91606-02-9; *rac*-Et[Ind]$_2TiCl_2$, 91685-21-1; Cp_2ZrCl_2, 1291-32-3; $(Me_5Cp)CpZrCl_2$, 81476-73-5; (*cis*-$CD_3CD{=}CHD$)-(propylene) (copolymer), 91586-05-9; propylene, 115-07-1; isotactic polypropylene (homopolymer), 25085-53-4; polypropylene (homopolymer), 9003-07-0.

Absolute Configurations, Maximum Rotations, and Kinetics of Thermal Racemization of the 1-Phenyl-2-deuteriocyclopropanes

John E. Baldwin*† and Timothy C. Barden

Contribution from the Department of Chemistry, University of Oregon, Eugene, Oregon 97403.
Received March 29, 1984

Abstract: From precursors of known absolute configurations and optical purities have been prepared (1*S*,2*R*)-(−)-*cis*-1-phenyl-2-deuteriocyclopropane and the (1*R*,2*R*)-(+)-trans isomer. The predicted kinetics of racemization for the (−)-cis isomer at 309.3 °C based on the known rate constants for all four distinct modes of stereomutation interconverting 1-phenyl-1,2,3-trideuteriocyclopropanes have been experimentally confirmed, providing an independent validation of those rate constants and the mechanistically informative conclusion they support: one-center epimerizations are decisively dominant in the thermal stereomutations of phenylcyclopropane.

The thermal stereomutations of cyclopropanes[1] have been the subject of numerous experimental and theoretical studies since 1958, the year when Rabinovitch, Schlag, and Wiberg disclosed the thermal interconversion of *cis*- and *trans*-1,2-dideuteriocyclopropane.[2] At least three factors have sustained this unusually prolonged and intensive study of the reaction: it has relevance to the structure and chemistry of trimethylene, one of the simplest localized biradicals;[3] it involves a hydrocarbon small enough to be explored meaningfully by theoretical methods of reasonable

† Present address: Department of Chemistry, Syracuse University, Syracuse, NY 13210.

(1) For major reviews and references to early work in this area see: Berson, J. A. *Annu. Rev. Phys. Chem.* **1977**, *28*, 111-132. Berson, J. A. In "Rearrangements in Ground and Excited States"; de Mayo, P., Ed.; Academic Press: New York, 1980; Vol. 1, pp 311-334. Borden, W. T. In "Reactive Intermediates"; Jones, M.; Moss, R. A., Eds.; Wiley: New York, 1981; Vol. II, pp 176-188. Gajewski, J. J. "Hydrocarbon Thermal Isomerizations"; Academic Press: New York, 1981, pp 27-35. Dervan, P. B.; Doughterty, D. A. In "Diradicals"; Borden, W. T., Ed.; Wiley: New York, 1982; pp 107-149.

0002-7863/84/1506-6364$01.50/0